

## Evidence and Limits of Universal Topological Surface Segregation of Cyclic Polymers

Qiming He,<sup>1</sup> Shih-Fan Wang,<sup>1</sup> Renfeng Hu,<sup>5</sup> Bulent Akgun,<sup>2,3,4</sup> Caleb Tormey,<sup>5</sup> Somesh Peri,<sup>1</sup>  
David T. Wu,<sup>5</sup> and Mark D. Foster<sup>1,\*</sup>

<sup>1</sup>*Department of Polymer Science, The University of Akron, Akron, Ohio 44325-3909, USA*

<sup>2</sup>*Department of Chemistry, Bogazici University, Bebek, Istanbul 34342, Turkey*

<sup>3</sup>*NIST Center for Neutron Research, National Institute of Standards and Technology, Gaithersburg, Maryland 20899-6102, USA*

<sup>4</sup>*Department of Materials Science and Engineering, University of Maryland, College Park, Maryland, 20742, USA*

<sup>5</sup>*Chemical Engineering and Chemistry Departments, Colorado School of Mines, Golden, Colorado 80401, USA*

(Received 12 May 2016; revised manuscript received 14 December 2016; published 21 April 2017)

If you mix lines and circles, what happens at the edge of the mixture? The problem is simply stated, but the answer is not obvious. Twenty years ago it was proposed that a universal topological driving force would drive cyclic chains to enrich the surface of blends of linear and cyclic chains. Here such behavior is demonstrated experimentally for sufficiently long chains and the limit in molecular weight where packing effects dominate over the topological driving force is identified.

DOI: [10.1103/PhysRevLett.118.167801](https://doi.org/10.1103/PhysRevLett.118.167801)

Topological effects are difficult to handle in theoretical treatments of physical phenomena. Thus, when such effects are present they invite particular attention. Phenomena in which topological effects play a role include the quantum Hall effect [1], superconductivity [2], topological insulators [3], spin liquids [4], and defect behavior in crystals [5]. Because of the variety of and control over their connectivity, polymers are particularly interesting for exploring topological effects on physical properties, including polymer rheology [6–9] and thermodynamics [10–18]. In particular, polymer melts containing cyclic or long-branched chains have rheology and chain dynamics [13] that can differ dramatically with architecture and are different from those of linear analogs. The ordering of block copolymers [19] and the crystallization of chains [20] differ with chain topology as well.

The blending of polymers of different topologies presents opportunities for a universal strategy independent of monomer chemistry for tailoring both bulk and surface properties, since, in general, chains of one topology will be preferred at the surface over otherwise identical chains of a different topology [21]. As an example, addition of very small amounts of linear polymers into matrices of cyclic chains significantly alters the structure and dynamics of the cyclic polymer melts, as demonstrated by experiments and simulations [6–13, 19–20, 22]. To demonstrate or probe the topological effect requires controlling for other factors which could otherwise drive surface segregation. Surface segregation has generally been understood in terms of a surface potential or free energy preference for specific chemical groups or units on the polymer chain. An attractive surface potential for a particular unit then favors chain configurations with this unit at the surface, resulting in surface enrichment of the chain containing that group. Thus, differences in the segment unit chemistries of two

blend components occasion a strong enthalpic driving force for surface segregation. Using the deuterated and hydrogenous species of polystyrene reduces this driving force tremendously while preserving a contrast mechanism between the species [23–28]. In linear-linear blends, differences in chain length drive shorter chains to the surface. This can likewise be explained in terms of a surface potential for chain ends [28–32]. Differences in the end unit chemistries of two components, or ends on one component being strongly preferred at the surface could yield another enthalpic driving force [33, 34].

Surface segregation in polymer blends driven by chain topology is more difficult to describe theoretically than is enthalpically driven segregation. Both blends containing branched chains [14–17] and blends containing cyclic polymers [18] are of practical interest and the behaviors of these two sorts of topological blends are expected to be quite different. Advances in synthetic methods [35] provide means for engineering the degree to which these topological effects are important by varying not only the molecular architecture, but also the molecular weight,  $M$ .

Wu and Fredrickson [21] proposed that segregation of branched chains to the surface can be rationalized using linear response theory, in which the driving force can be simplified in terms of effective surface potentials for ends and branch points. The predictions are consistent with self-consistent field theory (SCFT) simulations and neutron reflectivity (NR) results by Mayes and co-workers [14, 36] and Foster and co-workers [15, 17] for branched chains of varying architecture. However, this simple approach is unable to capture behaviors that can be observed in blends containing cyclic chains, which lack ends and branch points.

Using an analytical linear response SCFT valid at high molecular weights, Wu and Fredrickson [21] analyzed the

entropic penalty for placing cyclic chains at a surface as compared to linear chains. Both cyclic chains and linear chains lose possible configurations when drawn to a surface from the bulk, but the cyclic chains lose fewer as they are already constrained in the bulk. This mechanism for enriching cyclics at the surface cannot be described simply with a surface potential, in contrast to the case of branched chains. Furthermore, for dilute cyclic chains in much longer linear chains, the surface concentration of cyclics is predicted to be double the bulk concentration, independent of  $M$ . A consequence of this is that the integrated surface excess increases with  $M$  for cyclic chains, but is approximately constant for linear chains, emphasizing the differing underlying mechanisms in these two cases. This unusual universal enrichment factor and molecular weight independence for cyclics results from the reduced entropic penalty for placing cyclic chains at a surface as compared to linear chains.

In this Letter we present experimental evidence for this universal topological driving force for cyclic chains toward a surface, and find limits where this universal driving force is no longer dominant. We performed NR measurements of the excess density of cyclic chains at a free surface for a range of  $M$ . At  $M = 37k$ , cyclic chains are indeed enriched at the surface, and the density profile is well described by a SCFT which removes the linear response assumption of the theory of Wu and Fredrickson. However, as  $M$  is decreased, starting at a value of  $M$  of approximately  $16k$ , linear chains are enriched at the surface. We hypothesize that this crossover is due to the growing importance of detailed packing effects, such as steric exclusion, stiffness, and differences in molecular size, that are not captured in the SCFT. We furthermore present a wall polymer reference interaction site model (wall-PRISM) theory that incorporates packing effects able to rationalize the behavior at  $M = 2k$  [37,38].

Well-defined cyclic polystyrenes (hCPS) of high purity (>99.7%) required to define the variation in surface segregation with  $M$  due to topological effects were synthesized using anionic polymerization and metathesis ring closure [35], and characterized with size exclusion chromatography and matrix assisted laser desorption mass spectrometry (MALDI-TOF MS, Figs. S1-S4 [41]). There was no chemical functionality in the cyclic chain that could strongly drive surface segregation. Linear polystyrene (hLPS) analogs were synthesized using *sec*-butyllithium initiator and terminated with methanol. Anionically polymerized deuterated linear polystyrenes (dLPS) were purchased from Polymer Source [39]. For both hLPS and dLPS neither chain end is strongly attracted to the air surface. Molecular characterization results for hLPS, dLPS, and hCPS are summarized in Table I. Silicon substrates (EL-CAT Inc., 7.7 cm dia.) were cleaned with piranha solution [40] and the native oxide removed. Each film was spun cast onto an etched silicon wafer from a

TABLE I. Molecular characterization of polymers.

Polymer	$M_n^a$ (g/mol)	PDI <sup>a</sup>	$[\eta]^b$ (cm <sup>3</sup> /g)	$T_g^c$ (°C)
hLPS2k	2300	1.05	0.047	61
dLPS2k	2000	1.03	0.041	60
hCPS2k	2700	1.03	0.037	85
hLPS6k	6000	1.02	0.10	87
dLPS6k	6500	1.06		92
hCPS6k	6000	1.03	0.064	99
hLPS16k	16 000	1.02	0.15	99
dLPS16k	16 000	1.02		95
hCPS16k	16 600	1.06	0.088	99
hLPS37k	38 000	1.03	0.25	104
dLPS37k	37 000	1.01	0.25	104
hCPS37k	37 000	1.09	0.20	104

<sup>a</sup>Determined by size exclusion chromatography coupled with light scattering ( $\pm 5\%$ ) in THF at 30 °C.

<sup>b</sup>Determined in toluene at 30 °C ( $\pm 0.5\%$ ).

<sup>c</sup>Determined by DSC: heating rate: 10 °C/min, recording second run,  $\pm 1$  °C.

blend toluene solution containing  $19.6\% \pm 0.5\%$  volume fraction of the hydrogenous component. Films of blends of  $2k$ ,  $6k$ ,  $16k$ , or  $37k$  components were annealed at ca.  $1 \times 10^{-7}$  Pa and 120 °C (for  $2k$ ,  $6k$ , and  $16k$ ) or 180 °C (for  $37k$ ) for 12 h. Concentration depth profiles were inferred from NR measurements at the NG7 neutron reflectometer at the NIST Center for Neutron Research using scattering vector  $q_z$  values of 0.008 to  $0.2 \text{ \AA}^{-1}$  with a relative resolution  $\Delta q_z/q_z$  of 0.04. The composition depth profile was obtained by nonlinear least squares regression of the data with a constraint that the overall mass ratio of hydrogenous and deuterated species in the original blend was conserved to within 3% (see Supplemental Material, Fig S5 [41]).

Analyses of the NR measurements of a  $37k$  linear-linear blend and  $37k$  cyclic-linear blend [41] provide the concentration depth profiles shown in Fig. 1(a). In the linear-linear blend, the hydrogenous species is depleted at the blend surface, consistent with the observations by others [25] for similar molecular weight linear-linear blends. However, the surface of the  $37k$  cyclic-linear blend is substantially enriched by the hydrogenous cyclic species, despite the isotopic effect that works against the topologically driven surface segregation. The experimentally observed ratio of the cyclic surface volume fraction to bulk volume fraction is  $1.9 \pm 0.12$ , consistent with the predictions for a universal topological driving force. For cyclic PS chains,  $37k$  chains are already large enough to be difficult to make, and they provide for this study our test of the behavior for long chains.

For these longer chains, the SCFT treatment should be reasonably suited. The SCFT is a coarse-grained mean-field theory for the polymer density, which is assumed to be that of a single test chain moving in the self-consistent mean field due to the other chains. The conformational

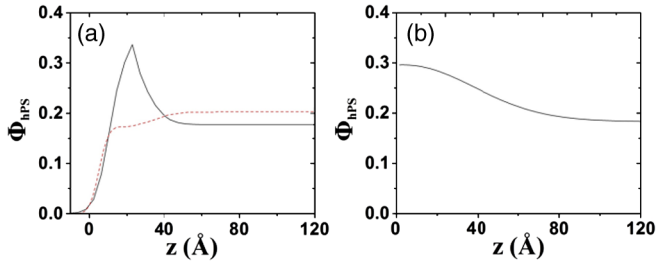


FIG. 1. (a) Experimentally measured hPS segment volume fraction depth profiles for the 37k cyclic-linear (solid curve) and 37k linear-linear (dashed curve) blend films after annealing at 180°C for 12 h. (b) Segment volume fraction depth profile for a 37k cyclic-linear blend with ideally smooth surface calculated using SCFT, with  $\varphi_{\text{cyclic}} = 0.2$ , total bulk segment density  $\rho_b = 1.0$ ,  $b = 6 \text{ \AA}$ , and  $v = 1b^3$ .

distributions of both linear and cyclic polymers are derived from the same two-point propagator,  $G(z, z'; t, t')$ , representing the statistical weight of a monomer  $t$  at position  $z$  connected by the chain to another monomer  $t'$  at position  $z'$ , since the chains are composed of the same monomers. The chains in the bulk are expected to obey random walk statistics at a coarse-grained level, and so the propagator obeys the modified diffusion equation

$$\partial G / \partial t = b^2 (\nabla^2 G) / 6 - \mu G, \quad (1)$$

where  $b$  is the statistical segment length. Moreover, the self-consistent potential is taken at a coarse-grained level to be proportional to the local monomer density, i.e.,  $\mu(z) = v\rho(z)$ , where  $v$  is the excluded volume parameter and  $\rho(z)$  the monomer density, can be expressed in terms of integrals over  $G$  [21]. Unlike in Ref. [21], no linear response approximation is made, and thus both finite cyclic concentrations and excluded volume parameters can be handled. These equations are numerically solved iteratively to convergence.

The composition profile for the 37k blend (without the isotopic labeling effect) from SCFT, shown in Fig. 1(b), predicts that  $\varphi_{\text{surface}}/\varphi_{\text{bulk}}$  should be about 1.6. The parameters chosen are close to values used in the literature ( $b = 6.8 \text{ \AA}$ ) [42], normalizing to the bulk density ( $\rho_b = 1.0$ ) and taking the excluded volume parameter to be on the scale of the monomer volume ( $v = 1b^3$ ). The result from this more detailed calculation is consistent with the earlier result from linear response theory [21]. The agreement with the experimental result is reasonably good, considering that the stiffness of the PS is not accounted for. However, for low  $M$ , local packing effects at the surface could be expected to become important [37–38,43].

For the cyclic-linear blend with the lowest  $M$ , the surface is enriched by the linear species [18], as shown in Fig. 2(a). While for the linear-linear blend the isotopic effect drives a weak enrichment of the surface with the deuterated linear

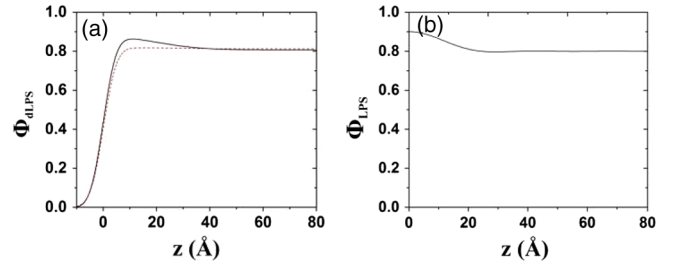


FIG. 2. (a) Comparison of linear dPS segment volume fraction depth profiles from NR for the 2k cyclic-linear blend film (solid curve) and 2k linear-linear blend film (dashed curve) after annealing at 120°C for 12 h. (b) Smoothed segment volume fraction profile for the 2k cyclic-linear blend with ideally smooth surface calculated using wall-PRISM with  $\varphi_{\text{cyclic}} = 0.2$ ,  $N = 20$  beads, total bulk segment density  $\rho_b = 1.0$ , packing fraction of 0.45, and 80/20 ratio of linear to cyclic polymers.

species, in the cyclic-linear blend this enrichment is strengthened further, which is counter to what would be expected from the SCFT [21]. Though TOF SIMS measurements are challenging to calibrate, they nonetheless corroborate the contention that the surface in the 2k case is enriched with dLPS and that the enrichment is stronger when the hydrogenous species is the cyclic chain [18]. Further investigation using Surface Layer MALDI-TOF MS provides a ratio of the cyclic surface volume fraction to bulk volume fraction of  $0.54 \pm 0.14$ , which is in quantitative agreement with the NR result [18].

It is difficult to capture both topological effects and local packing effects in one theory to explain the behavior for the entire range of  $M$ . SCFT could be expected to perform poorly in predicting the surface segregation behavior for short chains. Both the linear and cyclic short chains are non-Gaussian, but the cyclic chains more so. Packing effects near the surface should be important [37–38,43–44]. Recent molecular dynamics simulation study predicts a depletion of cyclic chains of low  $M$  at the surface due to the fact that a severe constraint is imposed on the flexibility of the cyclic chains when the chain length is small, which frustrates the packing of the cyclic chains at the surface. The linear chains can minimize their surface enthalpy more readily than can their cyclic counterparts when packing at the surface, and at the same time maximize their entropy by exposing chain ends towards the surface [43]. Therefore, the 2k case was investigated using wall-PRISM theory, which accounts for the presence of a surface using the polymer reference interaction site model theory for monomer density correlations expanded to include an infinitely large particle that provides the surface [35]. The wall-PRISM theory approximately captures the many-body effects of packing by recursively summing chains of interactions between “interaction sites,” which are the monomers or the wall particle, in calculating the probability of a monomer being a given distance from the wall. The 2k chains, which correspond to about 20 styrene monomers,

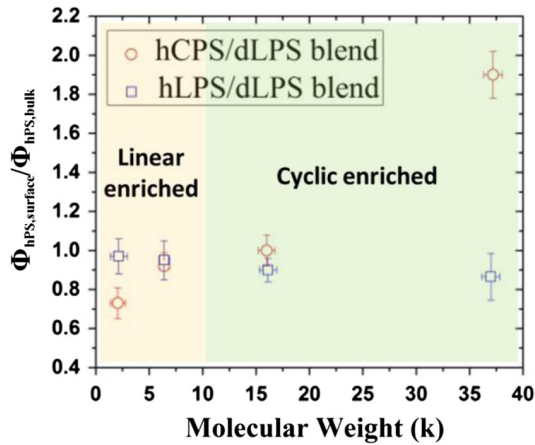


FIG. 3. Ratio of surface volume fraction to bulk volume fraction for hydrogenous cyclic and hydrogenous linear chains as a function of molecular weight.

were modeled as chains of 20 tangent spheres of diameter  $\sigma = 5 \text{ \AA}$ , which is on the order of the statistical segment length, and assuming a segment molecular weight of 100 g/mol (styrene is 104 g/mol). To compare with the experimental profile, the concentration depth profile found with a wall-PRISM calculation for the  $2k$  cyclic-linear blend was smoothed with a Hann resolution window (cosine lobe, with  $k_{\text{max}} = 1/4\sigma$  to match the resolution of the NR experiment). The result is shown in Fig. 2(b), and indeed it correctly predicts that the linear species should be mostly enriched at the surface.

The crossover in segregation behavior in going from the small  $M$  case to the large  $M$  case is intriguing. To identify more precisely this crossover, the ratio of surface volume fraction to bulk volume fraction was also determined experimentally for  $6k$  and  $16k$  cyclic-linear blends having also a small isotopic effect. Figure 3 shows that the ratio is still less than unity for the  $6k$  blend and then passes through unity at about  $M = 16k$ . Using the results found for the linear-linear analog blend as a measure of the isotopic effect present in the cyclic-linear blends, we estimate that in the absence of that isotopic effect the crossover from enrichment by linear chains to enrichment by cyclic chains would occur for  $M$  between  $10k$  and  $15k$ . This is in reasonable agreement with the estimate by Tsige and co-workers [43] from simulations that a crossover should occur between  $6k$  and  $10k$ . At the crossover  $M$ , the topological driving force, which pulls cyclic chains towards the surface, is balanced by the packing frustration, which depletes the cyclic chains from the surface.

In summary, experiments and theoretical study of surface segregation of cyclic-linear blends as a function of  $M$  provides experimental evidence for a universal topological driving force that cannot be described by conventional surface potentials, and a limit to the dominance of this force for shorter chains. We have shown experimentally that for sufficiently long chains, cyclics enrich the surface as a

result of a new topological driving force predicted 20 years ago using SCFT [21]. Linear polymers enrich the surface for short chains, consistent with wall-PRISM theory [37,38]. A crossover at  $M$  of  $10k$ – $15k$  in the absence of isotopic effects results from a balance between poorer packing of cyclic polymers at the surface and the smaller conformational entropy loss for bringing cyclics to the surface. These results are consistent with a crossover from a packing dominated surface enrichment to a topological mechanism. Measurements performed on even higher molecular weight chains will help confirm this interpretation. These competing driving forces enable us to tailor the surface composition of a cyclic-linear blend, and provide us with the opportunity to access desired properties by tuning  $M$  for both cyclic and linear chains. Moreover, the topological driving force at high  $M$  presents opportunities for exploration of other looped topologies, such as cloverleaf or linked ring topologies, as well as exploitation for surface enrichment applications.

This work was supported by NSF Grants No. CBET-0730692 and No. CBET-0731319. We acknowledge the support of the National Institute of Standards and Technology, U.S. Department of Commerce, in providing the neutron research facilities used in this work.

Q. H. and S.-F. W. contributed equally to this work.

\*Corresponding author.  
mfoster@uakron.edu

- [1] C. L. Kane and E. J. Mele, *Phys. Rev. Lett.* **95**, 146802 (2005).
- [2] M. Leijnse and K. Flensberg, *Semicond. Sci. Technol.* **27**, 124003 (2012).
- [3] H. Zhang, C. Liu, X. Qi, X. Dai, Z. Fang, and S. Zhang, *Nat. Phys.* **5**, 438 (2009).
- [4] X. G. Wen, *Phys. Rev. B* **44**, 2664 (1991).
- [5] I. Musevic, M. Skarbot, U. Tkalec, M. Ravnik, and S. Zumer, *Science* **313**, 954 (2006).
- [6] G. B. McKenna, B. J. Hostetter, N. Hadjichristidis, L. J. Fetters, and D. J. Plazek, *Macromolecules* **22**, 1834 (1989).
- [7] Y. Doi, K. Matsubara, Y. Ohta, T. Nakano, D. Kawaguchi, Y. Takahashi, A. Takano, and Y. Matsushita, *Macromolecules* **48**, 3140 (2015).
- [8] M. Kapnistos, M. Lang, D. Vlassopoulos, W. Pyckhout-Hintzen, D. Richter, D. Cho, T. Chang, and M. Rubinstein, *Nat. Mater.* **7**, 997 (2008).
- [9] J. D. Halverson, G. S. Grest, A. Y. Grosberg, and K. Kremer, *Phys. Rev. Lett.* **108**, 038301 (2012).
- [10] P. J. Mills, J. W. Mayer, E. J. Kramer, G. Hadziioannou, P. Lutz, C. Strazielle, P. Rempp, and A. J. Kovacs, *Macromolecules* **20**, 513 (1987).
- [11] D. G. Tsilikis and V. G. Mavrantzas, *ACS Macro Lett.* **3**, 763 (2014).
- [12] S. Habuchi, N. Satoh, T. Yamamoto, Y. Tezuka, and M. Vacha, *Angew. Chem., Int. Ed.* **49**, 1418 (2010).
- [13] S. Gooßen, M. Krutyeva, M. Sharp, A. Feoktystov, J. Allgaier, W. Pyckhout-Hintzen, A. Wischniewski, and D. Richter, *Phys. Rev. Lett.* **115**, 148302 (2015).

- [14] D. G. Walton, P. P. Soo, A. M. Mayes, S. J. Sofia Allgor, J. T. Fujii, L. G. Griffith, J. F. Ankner, H. Kaiser, J. Johansson, G. D. Smith, J. G. Barker, and S. K. Satija, *Macromolecules* **30**, 6947 (1997).
- [15] M. D. Foster, C. C. Greenberg, D. M. Teale, C. M. Turner, S. Corona-Galvan, E. Cloutet, P. D. Butler, B. Hammouda, and R. P. Quirk, *Macromol. Symp.* **149**, 263 (2000).
- [16] I. Mitra, X. Li, S. L. Pesek, B. Makarenko, B. S. Lokitz, D. Uhrig, J. F. Ankner, R. Verduzco, and G. E. Stein, *Macromolecules* **47**, 5269 (2014).
- [17] J. S. Lee, N. H. Lee, S. Peri, M. D. Foster, C. F. Majkrzak, R. Hu, and D. T. Wu, *Phys. Rev. Lett.* **113**, 225702 (2014).
- [18] S. Wang, X. Li, R. L. Agapov, C. Wesdemiotis, and M. D. Foster, *ACS Macro Lett.* **1**, 1024 (2012).
- [19] B. V. S. Iyer, A. K. Lele, and S. Shanbhag, *Macromolecules* **40**, 5995 (2007).
- [20] S. Honda, M. Koga, M. Tokita, T. Yamamoto, and Y. Tezuka, *Polym. Chem.* **6**, 4167 (2015).
- [21] D. T. Wu and G. H. Fredrickson, *Macromolecules* **29**, 7919 (1996).
- [22] N. Sugai, S. Asai, Y. Tezuka, and T. Yamamoto, *Polym. Chem.* **6**, 3591 (2015).
- [23] R. A. L. Jones, E. J. Kramer, M. H. Rafailovich, J. Sokolov, and S. A. Schwarz, *Phys. Rev. Lett.* **62**, 280 (1989).
- [24] R. A. L. Jones, L. J. Norton, E. J. Kramer, R. J. Composto, R. S. Stein, T. P. Russell, A. Mansour, A. Karim, G. P. Felcher, M. H. Rafailovich, J. Sokolov, X. Zhao, and S. A. Schwarz, *Europhys. Lett.* **12**, 41 (1990).
- [25] A. Hariharan, S. K. Kumar, M. H. Rafailovich, J. Sokolov, X. Zheng, D. Duong, S. A. Schwarz, and T. P. Russell, *J. Chem. Phys.* **99**, 656 (1993).
- [26] J. Genzer, A. Faldi, and R. J. Composto, *Phys. Rev. E* **50**, 2373 (1994).
- [27] J. Genzer, A. Faldi, R. Oslanec, and R. J. Composto, *Macromolecules* **29**, 5438 (1996).
- [28] A. Hariharan, S. K. Kumar, and T. P. Russell, *J. Chem. Phys.* **98**, 4163 (1993).
- [29] A. Hariharan, S. K. Kumar, and T. P. Russell, *Macromolecules* **23**, 3584 (1990).
- [30] A. Budkowski, U. Steiner, and J. Klein, *J. Chem. Phys.* **97**, 5229 (1992).
- [31] P. Cifra, F. E. Karasz, and W. J. MacKnight, *Macromolecules* **25**, 4895 (1992).
- [32] P. P. Hong, F. J. Boerio, and S. D. Smith, *Macromolecules* **27**, 596 (1994).
- [33] D. R. Iyengar, S. M. Perutz, C. Dai, C. K. Ober, and E. J. Kramer, *Macromolecules* **29**, 1229 (1996).
- [34] T. F. Schaub, G. J. Kellogg, A. M. Mayes, R. Kulasekera, J. F. Ankner, and H. Kaiser, *Macromolecules* **29**, 3982 (1996).
- [35] R. P. Quirk, S. Wang, M. D. Foster, C. Wesdemiotis, and A. M. Yol, *Macromolecules* **44**, 7538 (2011).
- [36] D. G. Walton and A. M. Mayes, *Phys. Rev. E* **54**, 2811 (1996).
- [37] A. Yethiraj and C. K. Hall, *J. Chem. Phys.* **95**, 3749 (1991).
- [38] A. Yethiraj, *Chem. Eng. J. (Lausanne)* **74**, 109 (1999).
- [39] Certain commercial equipment, instruments, or materials (or suppliers) are identified in this Letter to foster understanding. Such identification does not imply recommendation or endorsement by the National Institute of Standards and Technology, nor does it imply that the materials or equipment identified are necessarily the best available for the purpose.
- [40] Piranha solution must be handled with care. Proper protective gear must be worn.
- [41] See Supplemental Material at <http://link.aps.org/supplemental/10.1103/PhysRevLett.118.167801> for reflectivity curves and fits.
- [42] *Polymer Handbook*, 2nd ed., edited by J. Brandrup and E. H. Immergut (Wiley and Sons, New York, 1975).
- [43] G. Pellicane, M. Megnidio-Tchoukouegno, G. T. Mola, and M. Tsige, *Phys. Rev. E* **93**, 050501 (2016).
- [44] E. Lee and Y. Jung, *Soft Matter* **11**, 6018 (2015).